Check for updates

Received: 16 January 2024 | Revised: 19 April 2024 | Accepted: 10 June 2024
DOI: 10.1002/hyp.15216

RESEARCH ARTICLE

WILEY

Combined effects of rainfall-runoff events and antecedent soil moisture on runoff generation processes in an upland forested headwater area

Tomáš Vichta[1] | Jan Deutscher[2] | Ondřej Hemr[2] | Gabriela Tomášová[1] | Nikola Žižlavská[3] | Martina Brychtová[2] | Aleš Bajer[1] | Manoj Kumar Shukla[4]

[1]Department of Geology and Soil Science, Faculty of Forestry and Wood Technology, Mendel University in Brno, Brno, Czech Republic

[2]Department of Landscape Management, Mendel University, Faculty of Forestry and Wood Technology, Mendel University in Brno, Brno, Czech Republic

[3]Department of Forest Management and Applied Geoinformatics, Mendel University, Faculty of Forestry and Wood Technology, Mendel University in Brno, Brno, Czech Republic

[4]Department of Plant and Environmental Sciences, College of Agricultural, Consumer and Environmental Sciences, New Mexico State University, Las Cruces, New Mexico, USA

Correspondence
Tomáš Vichta, Department of Geology and Soil Science, Faculty of Forestry and Wood Technology, Mendel University in Brno, Zemědělská 3, 61300 Brno, Czech Republic.
Email: tomas.vichta@mendelu.cz

Funding information
Internal Grant Scheme of Mendel University in Brno, Grant/Award Number: CZ.02.2.69/0.0/0.0/19_073/0016670

Abstract

In this study, we investigate the combined effect of different rainfall-runoff event types and antecedent soil moisture (ASM) on runoff processes in the headwater elementary discharge area of a small forested upland catchment. The study focuses on (i) the relationship between soil moisture thresholds and runoff generation; (ii) the combined effect of ASM and tree vicinity and (iii) the relationship between different rainfall-runoff event types and different types of runoff (baseflow and stormflow). The results suggest that ASM has a strong impact on local runoff generation processes. Soil water content (35%–36%) threshold exceedance was related to stormflow runoff generation caused by the activation of quick preferential flow paths in the soil during storm events, especially in the upper and the deepest soil layers. At the same time, unexpected non-linear increases in baseflow runoff ratios were documented during dry, precipitation-free, periods and when the 31%–34% soil moisture threshold was exceeded, presumably due to the hydrological connection of farther slope areas during these conditions. Multiple stormflow periods, which exhibited the lowest runoff coefficient, were the most significant events in terms of water retention and soil water recharge due to increased vertical hydrological connectivity enabling more rapid transport to deeper soil layers. However, this rainfall type occurred least often over the study period. The important role of forest stands (individual trees) in creating spatial patterns of soil moisture and preferential infiltration paths to deeper soil layers was also confirmed. These results contribute towards a better conceptualisation of hydrological behaviour in elementary headwater discharge areas and highlight the potential dangers associated with expected increases in extreme weather events.

KEYWORDS
baseflow, soil moisture threshold, stormflow, subsurface flow, weather extremes

This is an open access article under the terms of the Creative Commons Attribution License, which permits use, distribution and reproduction in any medium, provided the original work is properly cited.
© 2024 The Author(s). *Hydrological Processes* published by John Wiley & Sons Ltd.

1 | INTRODUCTION

Hydrological and geomorphological systems display distinctly different behaviours in response to certain thresholds. In runoff generation, such thresholds mainly become significant when separating quick and slow flow paths during and after precipitation events (Schellekens et al., 2004). These values, and the associated runoff processes, occur at different levels of complexity (Zehe & Sivapalan, 2009), both over spatial scales and with regard to hydrological return times (Norbiato & Borga, 2008; Zehe et al., 2007). Advancing climate change is expected to alter hydrological processes across the world's ecosystems, including forests. Understanding these thresholds, therefore, will be critical for correctly interpreting current and future runoff responses at individual watershed levels (Tetzlaff et al., 2008).

Soil moisture is a commonly recognized hydrologic variable that is often non-linearly related to runoff. However, previous studies (Brocca et al., 2005; James & Roulet, 2007; Penna et al., 2011; Radatz et al., 2013; Western & Grayson, 1998) have noted different soil moisture thresholds (23%–45%) in relation to the generation of stormflow runoff, probably due to differences in soil properties, depth and land use. At the same time, Tromp-van Meerveld and McDonnell (2006) and Radatz et al. (2013) reported that significant stormflow subsurface runoff occurs when precipitation exceeds a certain threshold, and that subsurface stormflow is related to both antecedent soil moisture (ASM) and total precipitation. However, there is little experimental evidence documenting how more frequent, less intense, episodic precipitation events affect runoff. Consequently, a combination of hydrological approaches and techniques will be necessary to obtain a complete picture of the relationship between soil moisture, precipitation and different forms of runoff, including the delineation of stemflow infiltration hotspot areas or utilization of stable isotopes (Brammer & McDonnell, 1996; Metzger et al., 2021; Uchida et al., 2005) aimed at identifying subsurface preferential runoff pathways. In forested catchments, macropores (especially those exceeding 50 mm in diameter; Beven & Germann, 1982) are thought to play an essential role in the hydrologic response as they represent significant preferential pathways for stormflow runoff generation. (Beven & Germann, 1982; Bonell, 1993). Macropores are formed through the activity of soil fauna, root dynamics (growth, decay), layering of soil horizons, translocation of clay, erosive action of subsurface flow or a combination of the above (Beven & Germann, 1982; Jones, 1971; Juřička et al., 2022; Lal, 1987); consequently, there can be wide spatial variability in the occurrence of macropores at the slope and watershed scales (Brammer & McDonnell, 1996; Jones, 1971). Application of physical model approaches of threshold runoff generation processes can only be successful, however, with a good understanding of this variability.

Surface runoff processes have been relatively well-defined (Beven, 1989). Sidle et al. (1995), and subsoil runoff processes are becoming better understood as well (Weiler, 2016), generally concerned about the role of macropore flow. Thresholds themselves can be employed in three different approaches (Lee & Kim, 2020): (i) using rainfall quantity and intensity (Du et al., 2016), (ii) using soil moisture and antecedent soil moisture (Detty & McGuire, 2010) and (iii) using both rainfall and soil moisture index to attribute soil water storage (Farrick & Branfireun, 2014). The threshold approach depends on the precipitation properties and regional features of the study area (Detty & McGuire, 2010) and can be further improved with the use of more factors such as rainfall intensity and amount and antecedent soil moisture for runoff prediction (Radatz et al., 2013). Considerable research has been conducted on the hydrologic threshold behaviour of catchments, summarized by Wilson et al. (2017). Response thresholds are driven by many factors of the aquifer-soil-vegetation system (Chittolina et al., 2023): groundwater level (Guérin et al., 2019), landscape and topography, especially riparian zones (McGlynn & McDonnell, 2003), bedrock microtopography (Tromp-Van Meerveld & McDonnell, 2006), physical soil properties (Detty & McGuire, 2010) such as soil water repellency or macropore flow (Nyman et al., 2010) or vegetation feedback (Wei et al., 2020). According to Wei et al. (2020). the concept of threshold behaviour is expected to serve as a promising new tool, which can be applied to evaluate stormflow response to forest recovery following ecological disturbances. To our knowledge, experimental data from the approach combining precipitation with dense soil moisture network and streamflow measurements to define runoff generation thresholds are still rather rare, especially coming from temperate forests in the Central European region.

The non-linear response of soil moisture to runoff has been reported (McGlynn, 2005; Penna et al., 2011; Sidle et al., 2000) and shows that the impact of soil moisture on runoff generation is particularly significant in steep, wet watersheds with shallow soils, with topographic features playing a significant role in subsequent hydrological processes (i.e. where the soil moisture threshold is met most of the time). However, relatively flat floodplain areas closer to the stream will have a greater potential to reach maximum water saturation, and thus quickly supply water to the stream network, resulting in a rapid streamflow/runoff response in reaction to rainfall events. Areas closer to the stream tend to respond differently, and almost independently, from slope zones, with runoff typically forming first in areas around the stream. Soil water stored in the more remote slope zones will only be released under wetter conditions when the stream and slopes become hydrologically connected (McGlynn et al., 2004; Ocampo et al., 2006; Wenninger et al., 2004). Western and Grayson (1998) stated that hydrological connectivity, as defined by spatial patterns and their effect on hydrologic response, is relevant to many hydrological processes. Slope studies have revealed much about the mechanisms and role of pipe flow (flow from a lateral preferential soil path) and its role in causing in-slope runoff at specific locations (e.g. Carey & Woo, 2000; Roberge & Plamondon, 1987). For example, the ratio of pipe flow to total slope flow for each storm was found to increase as total rainfall increased (Kitahara et al., 1994; Kitahara & Nakai, 1992). Though previous studies have reported soil moisture thresholds in relation to runoff generation, we still lack a proper understanding of the separate involvement of trees in runoff processes at the micro-catchment scale, not least as forested watersheds show greater variability in soil hydrological properties than other watersheds with other land-use types (Roberts, 2000), which can translate into very different runoff response behaviours.

10991085, 2024, 6, Downloaded from https://onlinelibrary.wiley.com/doi/10.1002/hyp.15216 by Mendel University in Brno, Wiley Online Library on [30/06/2024]. See the Terms and Conditions (https://onlinelibrary.wiley.com/terms-and-conditions) on Wiley Online Library for rules of use; OA articles are governed by the applicable Creative Commons License

While the aforementioned studies have covered several topographic, climatic and land-use zones, upland forested headwater areas have yet to be considered, especially in the context of water retention and runoff generation. To help address this, the present study focuses on three main questions: 1) is there a soil moisture threshold in upland forested headwater areas that controls surface and subsurface runoff responses at the scale of the entire headwater area, 2) what is the combined effect of ASM, infiltration hotspot areas near-tree and precipitation on runoff processes, and 3) how do different precipitation event types affect runoff generation?

2 | MATERIALS AND METHODS

2.1 | Study area

The study area is located in the Kanice experimental forested catchment (0.65 km^2; Deutscher et al., 2016) in the uplands (altitude ranging from 290 to 370 m) of the Czech Republic (Figure 1). The location is characterized by a continental temperate forest climate with a mean annual temperature of 10°C and precipitation of 606 mm (over the 30-year climatic standard 1991–2020; Babice nad Svitavou climate station; Czech Hydrometeorological Institute, 2023). During the growing season in April–October, the temperature reaches 16.8°C and precipitation 427 mm. Over the last decade, since 2012 mean annual precipitation has been lower under 580 mm because of less winter precipitation. Precipitation during the growing season still reaches 427 mm. Over recent years, while the runoff coefficient in the study area has been very low, reaching just 4%–16% (Deutscher et al., 2021), storm events have been important sources of catchment runoff, contributing significantly to the local flow regime.

In this study, hydrometeorological measurements were taken in a headwater sub-catchment of the Kanice catchment (Figure 1), the overall sub-catchment having an area of 7.6 ha (11.7% of the total catchment), altitude ranging from 314 to 370 m (Table 1), N–NW orientation and slope inclination of 0.1–39° (0.002%–81%). The site is densely covered with forest, with stands aged 61–80 years and 41–60 years covering 45.5% and 32.7% of the area, respectively, managed as standard production forest. The dominant tree species are oak (*Quercus petraea* agg. [Mat.] Liebl.) and beech (*Fagus sylvatica* L.), with Scots pine (*Pinus Sylvestris* L.) and hornbeam (*Carpinus betulus* L.) subdominant, representing 27.4%, 28.5%, 13.8% and 12.5% of the tree species composition, respectively. The mean leaf area index (LAI) for these forest stands was 2.17 m^2/m^2, with minimal and maximal LAI values ranging from 1.55 to 3.74 m^2/m^2. Root density varies with distance from the tree and depth, with near-tree (NT) rooting decreasing from 153 pcs/m^2 to 23 pcs/m^2 with depth, and between-tree (BT) rooting decreasing from 119 pcs/m^2 to 3 pcs/m^2 with depth. Detailed distribution of root density varies with distance from the tree and depth is part of the Supplementary Material, see Table S1.

The bedrock consists of granodiorite with an irregular admixture of loess, with the depth of loess affecting the diversity of soil types. Soils in the study area range in depth from approximately 50 to 90 cm (Table 2) and are predominantly well-drained sandy

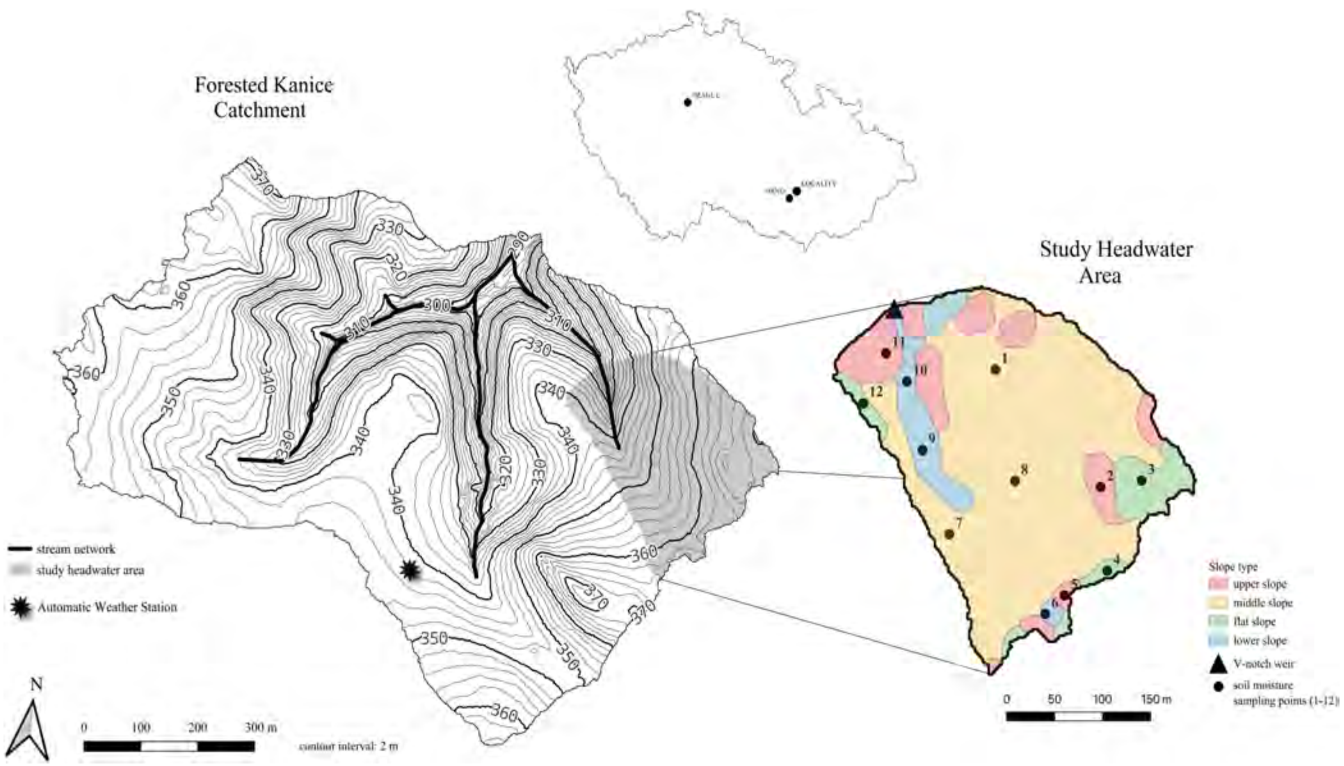

FIGURE 1 Location of the study area and instrumental design.

10991085, 2024, 6, Downloaded from https://onlinelibrary.wiley.com/doi/10.1002/hyp.15216 by Mendel University in Brno, Wiley Online Library on [30/06/2024]. See the Terms and Conditions (https://onlinelibrary.wiley.com/terms-and-conditions) on Wiley Online Library for rules of use; OA articles are governed by the applicable Creative Commons License

TABLE 1 Topographic and vegetation characteristic for soil monitoring points.

ID	Slope type (–)	Slope (°)	Aspect (°)	Altitude (m a.s.l.)	Main tree species (–)[a]	Stand age (years)	LAI (m^2/m^2)[b]	Root density (pcs/m^2)[c]
1	Middle slope	7.1	263	350	Beech, oak, hornbeam	78	2.81	229
2	Upper slope	16.5	232	368	Oak, hornbeam, beech	78	2.13	403
3	Flat slope	0.5	-	368	Oak, hornbeam	52	1.70	319
4	Flat slope	0.1	-	363	Oak, hornbeam	78	1.67	753
5	Upper slope	13.9	356	363	Oak, hornbeam	78	2.06	792
6	Lower slope	4.9	329	361	Oak, hornbeam, beech	81	2.03	226
7	Middle slope	5.0	357	352	Beech, hornbeam	28	2.82	274
8	Middle slope	5.5	265	355	Oak, beech, hornbeam	78	1.80	156
9	Lower slope	5.8	331	344	Hornbeam, beech, oak	78	1.91	98
10	Lower slope	4.1	360	332	Beech, hornbeam	81	1.64	137
11	Upper slope	10.0	26	334	Beech, hornbeam	17	2.36	164
12	Flat slope	0.6	-	341	Beech, hornbeam	17	3.10	161

[a]Main tree species in the vicinity of the soil probe (approx. 400 m^2, 20 × 20 m).
[b]Leaf area index determined according to hemispheric photography (digital camera with a fish-eye lens); images processing in WinSCANOPY software (Regent Instruments Inc., Canada).
[c]Plastic sheets were placed on the pit wall and a pen was used to mark clearly visible fine (<2-mm diameter) and thick roots (<2 mm), as described by Böhm (1979).

TABLE 2 Soil characteristics for soil monitoring points.

ID	Soil classification (–)[a]	Soil depth (cm)[b]	Texture (clay%–silt%–sand%)	Coarse fragments (%)	Soil organic carbon (%)[c]	Ration C/N (–)[c]	Ks (m/day)
1	luvic Cambisol	88	4–53–43	14.1	1.9	13.5	0.24
2	hyperskeletic Leptosol	55	3–49–48	75.5	6.3	15.2	5.38
3	skeletic Cambisol	52	3–47–50	33.4	3.4	13.5	6.31
4	skeletic Cambisol	65	4–42–54	46.8	4.0	13.0	5.82
5	hyperskeletic Leptosol	48	5–48–47	65.8	6.7	14.9	6.71
6	eutric Cambisol	83	6–39–55	33.2	2.3	15.1	0.49
7	skeletic Cambisol	79	3–39–58	33.7	1.6	14.8	2.46
8	eutric Cambisol	74	4–44–52	15.9	1.2	11.5	0.09
9	gleyic Stagnosol	94	4–55–41	7.9	1.4	9.4	0.16
10	gleyic Stagnosol	85	3–48–49	8.0	1.4	10.6	0.03
11	skeletic Cambisol	56	5–46–48	15.5	1.8	13.0	0.07
12	luvic Cambisol	74	4–51–42	2.9	2.0	12.3	0.15

[a]WRB system (2014).
[b]Subsoil and substratum boundary.
[c]Soil organic carbon and total nitrogen were assessed using a vario MACRO cube elemental analyser (Elementar, Germany).

loam (USDA, 1999) eutric Cambisols or luvic Cambisols altering with gleyic Stagnosols (WRB, 2014). The median saturated soil hydraulic conductivity (K_s) reaches 0.5 m/day over the entire soil profile and area. The soils in upper and flat slopes located in higher parts of the sub-catchment are well-drained (median $K_s = 3.4$ m/day) while soils in the lower parts closer to the stream are less so (median $K_s = 0.3$ m/day). Silt content decreases with depth from 52% to 32% and sand content increases with depth from 45% to 66%, while clay, as the least common component, ranges between 4% and 2%. Numerous macropore pathways were

10991085, 2024, 6, Downloaded from https://onlinelibrary.wiley.com/doi/10.1002/hyp.15216 by Mendel University in Brno, Wiley Online Library on [30/06/2024]. See the Terms and Conditions (https://onlinelibrary.wiley.com/terms-and-conditions) on Wiley Online Library for rules of use; OA articles are governed by the applicable Creative Commons License

observed in all soil profiles, even at the subsoil and substratum boundary, especially at NT sites. The substratum was considered to be either chemically and mechanically weathered bedrock or deluvial, solifluction and aeolian materials under the subsoil layer (below the B horizon).

2.2 | Determination of headwater area and instrumental design

The headwater area was first delineated on a freely available 2 × 2 m resolution digital terrain model (DTM) of the Kanice-forested catchment in ArcGIS v.10.6.1 (Esri, USA), after which the representative elementary area (REA) for the watershed (Wood et al., 1988) was distinguished from the DTM using the ArcGIS hydrology toolset (Esri, USA). This analysis, in combination with field surveys, allowed for the selection of a 'bowl'-shaped headwater source area of ca. 7.6 ha. Using the topographic position index tool (Guisan et al., 1999), the REA was then divided into four zones according to slope type (Weiss, 2001): upper slope = top part of the hillslope, >10°; middle slope = middle part of the hillslope, >5°; flat slope = the plateau on the hilltop, <5°; lower slope = lowest part of the hillslope, <5° (Figure 1); onto which an irregular 12-point grid was laid out for soil moisture monitoring. These zones then served as the methodological basis for the capture of all hill slope hydrological units. Finally, a 13th point was established at the outlet of the stream for streamflow measurements.

2.3 | Precipitation, streamflow and soil moisture monitoring

Precipitation, streamflow and soil moisture data were collected during the 2022 growing season, which lasted from April 1 to October 31. Precipitation was measured at 15-min intervals using an AMET automatic rain gauge (Litschmann and Suchý, Czech Republic) at a nearby (approx. 0.4 km) meteorological station. Streamflow was estimated from water level readings above a Thomson spillway (V–notch weir) at the catchment outlet. The weir was installed ca 20 m downstream of where the thalweg first changed into a characteristic stream bed. Measurements were carried out using a US3200 ultrasonic sensor combined with a HYDRO-LOGGER H_2 data logger (Fiedler Automatic Monitoring Systems AMS, Czech Republic), a 6 m × 4 m × 2 m roof being installed over the spillway to prevent objects (leaves, branches, etc.) falling into the stream and causing erroneous readings. Water level values were automatically converted to streamflow by the data logger every 15 min using the conversion curve for the Thomson spillway (Deutscher et al., 2021).

Soil water content (SWC) was measured over the irregular 12-point grid on each slope type, with each point comprising paired monitoring of NT and BT soil moisture. The sensors at the NT position were located 50 cm downslope of the tree trunk, while those at the BT position were located in the nearest crown gap, on the same contour as the NT probes. SWC was only measured in stands with deciduous tree species, that is beech, hornbeam and oak (Table 1) that were considered similar tree species for this study. The analysis was based on the combined effects of the mixed deciduous stands rather than the individual effects of different tree species. SWC was monitored on all slope types at 0–30 cm, supplemented by measurements at 30–60 cm for middle and flat slopes, and 30–100 cm for lower slopes. Paired SWC monitoring was repeated three times for each slope type, with 4–8 sensors per point, depending on slope type (soil depth), giving a total of 72 sensors over the study area. The SWC was then measured continuously at 15-min intervals using a TMS-4 microclimate datalogger (Wild et al., 2019), with each sensor calibrated for local soil conditions at each point and depth, based on soil particle size distribution and bulk density assessed from 60 soil samples previously taken from the area. The TMS Calibr utility (Wild et al., 2019), as supplied by the manufacturer, was used to calibrate all sensors.

2.4 | Selection of rainfall-runoff events

In total, 35 intermittent no-rainfall periods and 45 rainfall-runoff events occurred over the growing season. For the purposes of evaluating catchment response to different rainfall types and the influence of ASM on runoff processes, these periods were sub-divided to meet specific criteria as follows:

A. precipitation-free period: (i) zero precipitation, (ii) insignificant change in SWC at a depth of 10 cm (i.e. < 0.2% within intraday variation), (iii) ends with a precipitation event.
B. baseflow dominated regime: (i) rainfall occurred, (ii) no significant change in SWC at a depth of 10 cm, (iii) ends with 194 consecutive zero rainfall records (i.e. 48 h after the last rainfall event).
C. single stormflow events: (i) rainfall occurred, (ii) significant change in SWC at a depth of 10 cm during one rainfall record (>0.2%), (iii) an increase in SWC occurred at all depths (0–100 cm) in the NT position, (iv) ends with 194 consecutive zero rainfall records (i.e. 48 h after the last rainfall event).
D. multiple stormflow events: (i) rainfall occurred, (ii) significant change in SWC at a depth of 10 cm during two consecutive rainfall events (%), (iii) an increase in SWC occurred at all depths (0–100 cm) in the NT position, (iv) ends with 194 consecutive zero rainfall records (i.e. 48 h after the last rainfall event).

Following Sumner (1999), a period of 48 h, or 2 days after the end of a rainfall event, was set as a common time frame during which the rainfall effect on runoff could be observed under similar conditions. This was further supported by direct measurements of soil-saturated hydraulic conductivity in the study area, which reached 0.5 m/day.

2.4.1 | Determining runoff coefficients

For each rainfall-runoff event, the extent to which the soil had been wetted or drained and the ratio of stormflow runoff and baseflow were assessed and used to indicate different behaviours during

10991085, 2024, 6, Downloaded from https://onlinelibrary.wiley.com/doi/10.1002/hyp.15216 by Mendel University in Brno, Wiley Online Library on [30/06/2024]. See the Terms and Conditions (https://onlinelibrary.wiley.com/terms-and-conditions) on Wiley Online Library for rules of use; OA articles are governed by the applicable Creative Commons License

different hydrological regime types. For each event, the hydrograph was separated into baseflow and stormflow runoff using the constant-k method proposed by Blume et al. (2007). Runoff coefficients for A events (precipitation-free periods) were calculated from the rainfall of antecedent B, C or D events and the baseflow of the actual A event.

2.4.2 | Determination and analysis of inter-day SWC dynamics

For each rainfall-runoff event (B, C, and D), the inter-day SWC dynamics (increments and decrements) were calculated from daily averages as the difference between values on a specific day and the day before ($t - t_{n-1}$). The values were then used to express the sum of cumulative SWC decreases/increases for the entire event period. The series of daily decreases/increases were tested for normality using the Shapiro–Wilk test, after which the Student's t-test was applied for series pairs (NT $\times$ BT) with normal distribution, and the non-parametric Wilcoxon test if at least one of the soil moisture sets failed normality.

2.4.3 | Determining SWC threshold for runoff generation

There is currently no uniform methodological approach for defining SWC thresholds, thus both arbitrary assessments of the relationship between runoff and soil moisture and various statistical approaches are commonly used. In this study, we took an arbitrary approach, based on the relationship between runoff coefficients (baseflow and stormflow) as indicators of different runoff regimes and hydrological processes and ASM as an indicator of the antecedent conditions. Because of the differing duration of each event (0.1–11 days), mean daily baseflow values were used to enable mutual comparison. Since stormflow runoff duration never exceeded 24 hrs, however, no time corrections were applied and the 15-min intervals were used. As such, presented baseflow values are not affected by diurnal variations caused by transpiration dynamics, while the stormflow could be (more about this in the discussion).

We estimated the SWC threshold for stormflow and baseflow generation according to criteria indicative of threshold excess, based on: (i) median of the runoff coefficients in different rainfall-runoff event types (A, B, C and D), and (ii) the variance of runoff coefficient values occurring in adjacent SWC intervals. In this step, we were looking for non-linear behaviour indicative of the activation of different runoff-generating mechanisms (Scaife et al., 2020). Once the median was exceeded, if the variance dramatically increased (drying in A and B events) or decreased (wetting in C and D events) inside a SWC interval, the adequate soil moisture was considered indicative of a threshold. Decreases/increases of runoff coefficient values were tested by multiple F-test, at a significance level of $p < 0.15$, see Table S2. All statistical analyses were performed using R software (R version v.4.2.1 GUI 1.79 High Sierra build and RStudio v.2022.07.2 + 576; R Core Team, 2017).

3 | RESULTS

3.1 | Streamflow and precipitation time series

Total precipitation over the 2022 vegetation period was 432.8 mm (Table 3), which corresponds with the long-term average for the same period of 427 mm (precipitation for 1991–2020 from the Babice nad Svitavou climate station; CHMI, 2023). The growing season in 2022 can thus be considered as a representative of a standardly wet year. The antecedent year 2021 was very similar in terms of rainfall (415 mm during the growing season) while 2020 was extremely wet (more than 610 mm during the growing season). Mean rainfall-runoff event lengths ranged from 2.6 to 3.1 days, with A, B and C events being regularly distributed throughout the growing season. Daily precipitation differed with event type, with A, B and C events having values of 1.15, 4.24 and 11.99 mm/day, respectively. Total runoff from the area was only 10.5 mm, corresponding to 2.4% of total precipitation (of which 0.1% was stormflow runoff), indicating that the area has a low hydrological response to rainfall-runoff events and high retention capacity and water usage.

In general, stormflow runoff, which accounted for 4.7% of total runoff, was highly reactive throughout the study period (Figure 2), but especially over the short duration of precipitation events (Table 3). While stormflow runoff was highest for D events, when it accounted for 33.7% of total runoff, such events only covered 7.2% of the growing season. In comparison, non-precipitation A events were most represented (42.1%), followed by B events (32.1%), during which time stormflow runoff accounted for just 0.7% of total runoff. C events were most evenly distributed in terms of frequency during the study period (18.6%) and exhibited the second highest stormflow runoff at 9.3%.

While the mean duration of each event type was similar, there was a significant difference in both total runoff and runoff coefficients (Table 3). Interestingly, the overall runoff coefficient was highest for B events (baseflow hydrological regime), while lowest runoff coefficients were recorded during D events (multiple stormflow events), i.e. lowest drainage occurred during D events and highest during B events, in the form of baseflow. Runoff coefficients were highly variable over the study period, with coefficients of variation (CV) often exceeding 1 (Table 3). This variability tended to increase with total rainfall and event duration. In many cases, these rainfall-runoff events were also followed by a steady increase in streamflow that lasted deep into the no-rainfall A events, especially at the beginning and end of the growing season.

3.2 | Soil moisture time series

Mean SWC (for both NT and BT positions) at depths of 10, 30, 60, 100 cm was 29.9%, 28.2%, 31.2% and 34.5%, respectively (Figure 3). However, NT SWC was 5.0, 2.3 and 5.3% lower than BT values at 10, 30 and 60 cm, respectively, but 8.4% higher at 100 cm. Highest SWC (36.2%) was recorded during C and D events at 100 cm, while the lowest SWC readings (27.3%) were obtained during A

10991085, 2024, 6, Downloaded from https://onlinelibrary.wiley.com/doi/10.1002/hyp.15216 by Mendel University in Brno, Wiley Online Library on [30/06/2024]. See the Terms and Conditions (https://onlinelibrary.wiley.com/terms-and-conditions) on Wiley Online Library for rules of use; OA articles are governed by the applicable Creative Commons License

TABLE 3 Descriptive characteristic for precipitation-free periods (A) and rainfall-runoff events (B, C, D).

Parameter	A	B	C	D	Total
Quantity (n)	35	25	15	5	80
Duration in days (n)	90	69	40	15	214
Duration ratio (%)	42.1	32.1	18.6	7.2	100
Mean event length (days)	2.6	2.7	2.6	3.1	2.8
Rainfall (mm)	0.0	78.9	168.6	185.4	432.8
CV of rainfall (−)	-	8.34	6.74	4.04	9.40
Rainfall intensity (mm/day)	-	1.15	4.24	11.99	2.02
Runoff (mm)	4.08	3.25	2.09	1.06	10.48
CV of runoff (−)	0.37	0.30	0.82	1.50	0.75
Stormflow runoff (mm)	-	0.022	0.195	0.357	0.574
CV of stormflow runoff (−)	-	1.28	2.91	3.14	3.27
Runoff coefficient (mm/mm)	-	0.0412	0.0124	0.0057	0.0242
Stormflow runoff coefficient (mm/mm)	-	0.0003	0.0012	0.0019	0.0013
Stormflow runoff index (%)	-	0.7	9.3	33.7	5.5

Abbreviations: CV, coefficient of variance; Total, total over April–October vegetation season.

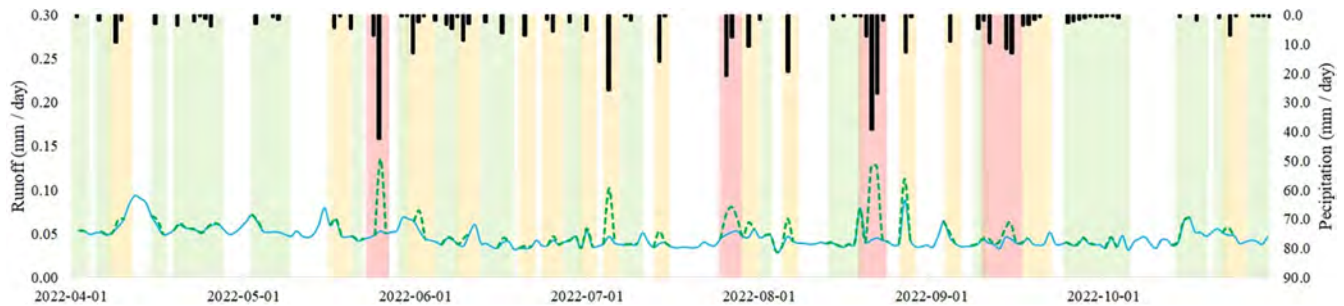

FIGURE 2 Daily time series of stormflow runoff (green line), baseflow (blue line) and precipitation (black bar) over the study period. Coloured bars represent periods with different rainfall-runoff events, where white = precipitation-free periods, green = baseflow dominated regime, yellow = single stormflow events, red = multiple stormflow events.

events at 30 cm. Highest and lowest relative SWC differences were also recorded during D events, with NT SWC being 13.3% higher at 100 cm, but 0.3% lower at 30 cm. In general, SWC dynamics during D events were more variable, with a high CV of 0.9. In comparison, C events had a CV of 0.6, with A and B events having identical CVs of 0.2. Overall, A and B events behaved linearly while C and D events behaved non-linearly.

Across the depth gradient, average daily decreases (A, B events) and increases (C, D events) in SWC showed similar patterns for soil drying and wetting (Table 4), though variability in drying/wetting increased with total rainfall. Unexpectedly, highest CV was recorded during C events (4.3), the other events, including D events, having CVs with a maximum value of 2 in all soil layers. Largest daily SWC declines were observed in the top 10 and 30 cm of soil during A and B events, with values ranging from −0.53% to −0.14% daily SWC. In general, soil drying values during B events were around 0.09% lower than those during A events. Conversely, SWC increases during D events were 0.94% higher than those during C events, particularly in the 10 and 30 cm topsoil layer, where values were 1.70% and 1.23% higher, respectively, compared with 0.52 and 0.31% daily SWC in the deeper layers.

SWC dynamics differed between NT and BT soil positions. In general, for A and B events, tree vicinity did not play a significant role in SWC, with similar values recorded at both positions and, with the exception of the topmost soil layer (10 cm), which showed a (non-significant) decrease in daily SWC from 0.11% to 0.06%, values tended to behave (decrease) similarly. During C and D events, however, SWC dynamics in NT and BT soils differed, with the whole NT profile showing a 0.50% higher SWC increase than BT soils during D events. The most significant contribution to total soil wetting occurred at 100 cm, with daily NT SWC showing a 0.70% increase over BT soils, which only reached a total of 0.04% daily SWC. This was also shown by the flat peak in NT SWC at 100 cm (Figure 3), which occurred during all five D events and five out of 15 C events (respective totals of 10.85, 15.75, 16.32, 19.38 and 19.95 mm).

3.3 | Relationship between SWC and runoff

Stormflow threshold was estimated with the use of median runoff coefficients from all B, C and D events. The relationship between

10991085, 2024, 6, Downloaded from https://onlinelibrary.wiley.com/doi/10.1002/hyp.15216 by Mendel University in Brno, Wiley Online Library on [30/06/2024]. See the Terms and Conditions (https://onlinelibrary.wiley.com/terms-and-conditions) on Wiley Online Library for rules of use; OA articles are governed by the applicable Creative Commons License

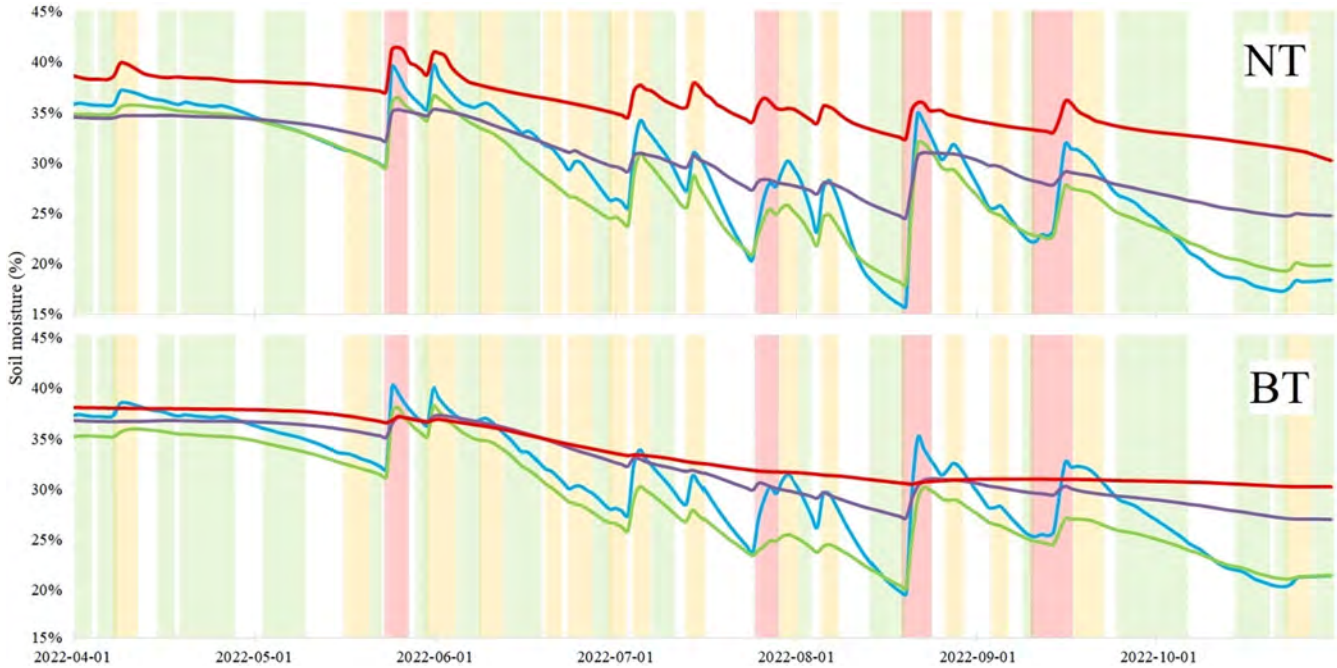

FIGURE 3 Daily time series for soil moisture at 10, 30, 60 and 100 cm (blue, green, violet and red lines, respectively) over the study period. Coloured bars represent periods with different rainfall-runoff events for near-tree soil (NT) and between-tree soil (BT), where white = precipitation-free periods, green = baseflow dominated regime, yellow = single stormflow events, red = multiple stormflow events.

TABLE 4 Daily drying (− SWC %) and re-wetting (+ SWC %) values for near-tree (NT) and between-tree (BT) soils over the study period: (A) precipitation-free periods, (B) baseflow dominated regime, (C) single stormflow event, and D) multiple stormflow event.

	A			B			C			D		
Depth	NT	BT		NT	BT		NT	BT		NT	BT	
10 cm												
Mean (%)	−0.53	−0.43	**	−0.28	−0.23	n.s.	+0.70	+0.43	*	+2.57	+2.02	*
CV (−)	0.9	0.8		1.1	1.5		1.5	1.5		0.6	0.6	
30 cm												
Mean (%)	−0.35	−0.25	***	−0.24	−0.14	*	+0.33	+0.49	n.s	+1.74	+1.22	n.s
CV (−)	0.7	0.7		0.9	2.3		2.5	3.1		0.8	0.9	
60 cm												
Mean (%)	−0.14	−0.10	***	−0.10	−0.07	***	+0.16	−0.03	n.s	+0.68	+0.40	n.s
CV (−)	0.7	0.7		0.8	0.8		4.3	3.9		1.1	1.1	
100 cm												
Mean (%)	−0.18	−0.05	***	−0.21	−0.04	***	+0.15	−0.04	n.s	+0.70	+0.04	*
CV (−)	1.4	1.0		1.6	1.2		2.9	1.6		0.8	2.0	

Note: Paired *T*-test: n.s = non-significant at $p < 0.05$; *, **, ***, significant at $p < 0.05$, $p < 0.01$, $p < 0.001$, respectively. CV = coefficient of variance; Number of repetitions at 10 cm: $N = 12$; 30 cm: $N = 12$; 60 cm: $N = 6$; 100 cm: $N = 3$.

ASM from 0 to 100 cm and stormflow runoff for the 45 rainfall-runoff events over the study period indicated an SWC threshold of about 35%–36% (Figure 4a,b). Once the threshold was exceeded, the stormflow runoff coefficient exhibited a non-linear increase above the median for B events (Figure 4a) and a nonlinear decrease for C and D events (Figure 4b).

Further analysis of ASM against median baseflow runoff coefficients from all events 25 B, 15 C and 5 D storm rainfall-runoff events (Figure 5a) and the 34 subsequent precipitation-free A events (Figure 5b) allowed for the identification of two further SWC thresholds beyond which baseflow started to increase non-linearly. Both thresholds were estimated at a similar value of around 31–34% SWC. Although rainfall totals were highest during D events, runoff coefficients never exceeded a median runoff coefficient of 0.007 mm/mm, especially during the following non-precipitation A events (median runoff

10991085, 2024, 6, Downloaded from https://onlinelibrary.wiley.com/doi/10.1002/hyp.15216 by Mendel University in Brno, Wiley Online Library on [30/06/2024]. See the Terms and Conditions (https://onlinelibrary.wiley.com/terms-and-conditions) on Wiley Online Library for rules of use; OA articles are governed by the applicable Creative Commons License

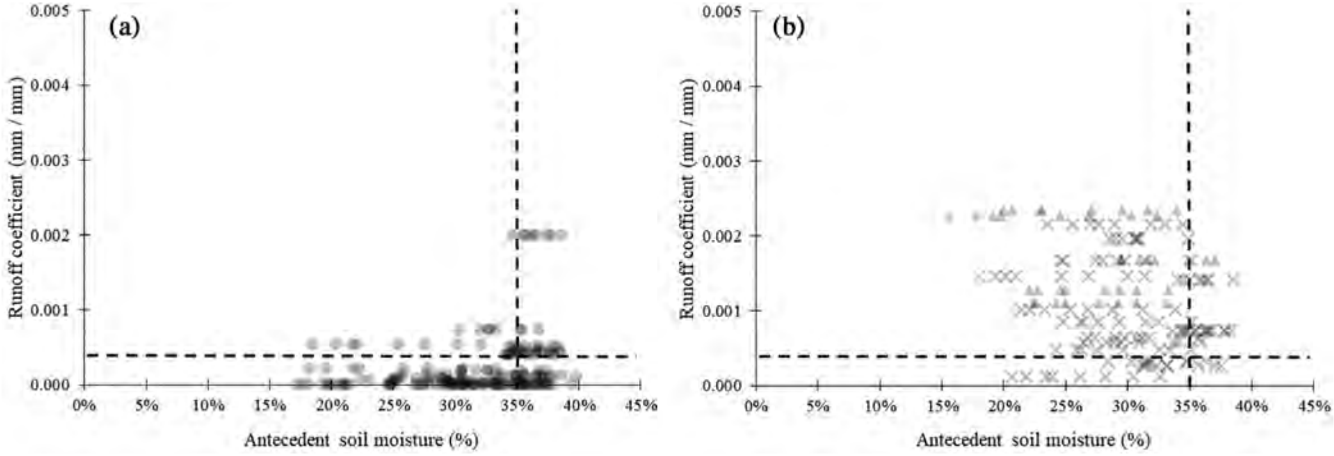

FIGURE 4 Threshold behaviour in the relationship between soil water content at 0–100 cm prior to the event and the stormflow runoff coefficient for (a) baseflow dominated regimes (B events; circles) and (b) single stormflow events (C events; crosses) and multiple stormflow events (D events; triangles). The horizontal line represents the stormflow runoff coefficient value compared to the median (0.0004 mm/mm).

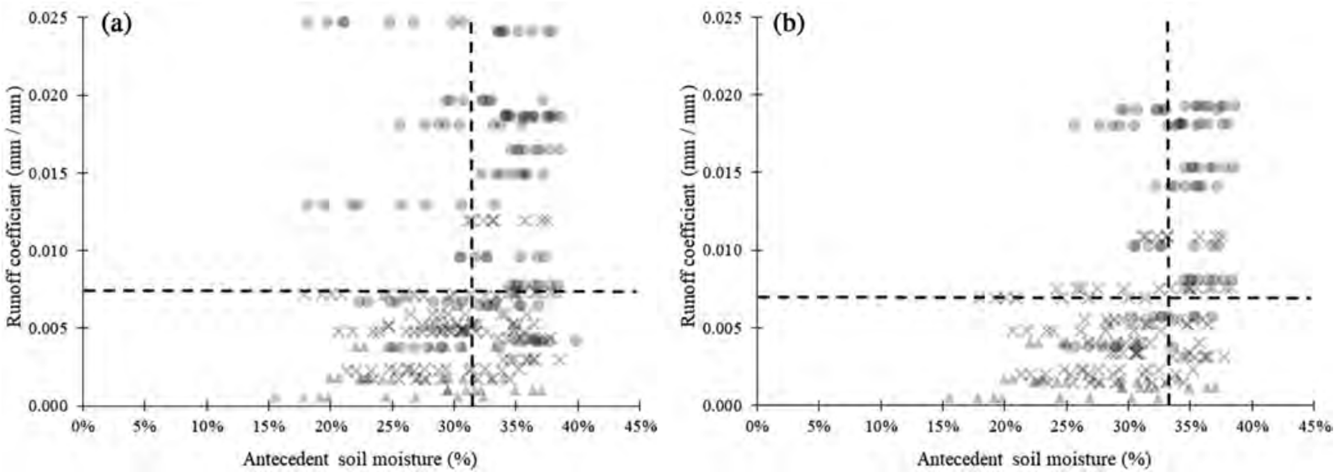

FIGURE 5 Threshold behaviour in the relationship between soil moisture at 0–100 cm prior to the event and (a) the runoff coefficient for baseflow in rainfall-runoff events and (b) the runoff coefficient for baseflow in no-rainfall-runoff events. Circles represent baseflow-dominated regimes, crosses represent stormflow events (C events) and triangles represent long-term stormflow events (D events). The horizontal line represents the value of the runoff coefficient corresponding to the medians of the B, C, D and A baseflow runoff coefficients (0.007 mm/mm).

coefficients of 0.007 mm/mm). Thus, the threshold was only approached during B and C events, indicating that D events contributed less to runoff, and more to catchment water retention, than C and B events.

4 | DISCUSSION

4.1 | Flow generation and subsurface processes

In this study, we examined the hydrology of a forested headwater catchment in an upland region of the Czech Republic where long-term annual precipitation was just 606 mm. This contrasts with similar previous studies that have usually been located in regions with higher annual precipitation of 820–1220 mm (James & Roulet, 2007; Radatz et al., 2013; Western & Grayson, 1998). In such areas, the emergence of fully saturated zones increases local reactivity, enabling the study of phenomena such as fill-and-spill (Tromp-Van Meerveld & McDonnell, 2006). In our case, however, the catchment was less saturated, hence we focused on SWC dynamics during rainfall-runoff events with different hydrological regimes. In doing so, the study can provide an illustrative example for other similar upland areas of Central Europe.

Periods of low soil saturation within the profile dominated throughout the April to October growing season and, consequently, streamflow response was limited due to poor hydrological connectivity. Overall, the dominant controlling factors for runoff were evapotranspiration processes and increased infiltration and transport of water from around trees into deeper layers through preferential subsurface flow along the roots. Detailed distribution of root density in

10991085, 2024, 6, Downloaded from https://onlinelibrary.wiley.com/doi/10.1002/hyp.15216 by Mendel University in Brno, Wiley Online Library on [30/06/2024]. See the Terms and Conditions (https://onlinelibrary.wiley.com/terms-and-conditions) on Wiley Online Library for rules of use; OA articles are governed by the applicable Creative Commons License

NT and BT soil is part of the Supplementary Material, see Table S1. In our study, we were able to demonstrate the significant role of trees for water transport through such soil layers during C and D events. These findings suggest an increased ability to transport water to lower layers at NT sites, especially during multiple stormflow D events. This is further supported by changes in SWC at 60 and 100 cm during C events, where NT soils had positive SWC values (+0.16 and +0.15%) and BT soils negative SWC values (−0.03% and −0.04%), suggesting that, under the same soil matrix conditions, wetting dominated over draining close to trees, while drying dominated over wetting in the gaps between trees.

Tromp-Meerveld and McDonnell (2005) found that there was a causal relationship between runoff threshold and active hydrological connectivity in forested landscapes. In their experimental watershed (Panola Mountain Research Watershed, USA), topsoil SWC was not a good indicator of when or where subsurface saturation would develop at the soil-subsoil interface on different slope types at sandy loam soils with little textural difference, ultimately leading to increased runoff generation once any depressions were filled. In our study, similar subsurface runoff patterns were also observed at the soil-subsoil interface, but in deeper soil layers and only around trees on similar textured soils (as indicated by higher wetting and flat SWC peaks at NT 100 cm) during all C and D events with rainfall intensity >10.75 mm/day.

In a second study, Tromp-Van Meerveld and McDonnell (2006) also found that, in general, vegetation affects spatial soil moisture patterns primarily through spatially dependent evapotranspiration. This was also confirmed in our headwater area, where temporary soil saturation only occurred in the uppermost soil layers (10 cm) and in the deepest soil layers (100 cm) at NT positions, where trees participate significantly in the formation of preferential runoff/infiltration paths, with no soil saturation in the rooting zone (30 and 60 cm). Spatial patterns controlled by higher evapotranspiration around trees were clearly demonstrated in our study through prominent inter-day SWC declines in NT soils during A events (conditions of low flow); NT inter-day SWC declines only being comparable to the upper layers of BT soils during B events (baseflow dominated conditions). As such, we assume that matrix flow over the entire soil profile only plays a limited role in runoff generation during unsaturated conditions (Beven & Germann, 2013), despite most hydrological concepts being based on this principle (Loague et al., 2006). Instead, we propose that the dominant role in runoff processes is given by preferential flow paths around trees. In the case of these preferential pathways, we observed non-linear SWC responses to rainfall events that we attribute mainly to root-induced bypass flow (Liang et al., 2011). At medium soil depths (30 to 60 cm), SWC dynamics were comparable at NT and BT sites, while significant increases in SWC were observed in the uppermost and deepest soil layers (10 and 100 cm) at NT sites. This 'bypass effect' was probably amplified by the relatively low precipitation rate over the study period (1.15–11.99 mm/day), which may have led to a proportionally higher interception rate, thereby increasing the stemflow that transports intercepted water to soil space below the tree (Staelens et al., 2008). This becomes particularly relevant where the dominant tree species are beech and hornbeam (Jochheim et al., 2022), whose effect on runoff generation will be most visible during low flow (A) and baseflow (B) conditions.

4.2 | Soil moisture threshold for runoff generation

While threshold soil moisture values have been reported in previous studies (e.g. Brocca et al., 2005; Radatz et al., 2013; Western & Grayson, 1998), they have so far been mostly viewed in relation to generation of stormflow runoff in fully saturated zones around streams characterized by high reactivity. During intense rainfall events, shallow subsurface flow in the upper soil profile layers (stormflow runoff) of well-drained slopes can be an important runoff mechanism (James & Roulet, 2007). However here, we show that, during the growing season of a standardly wet year in our forested study headwater area, only less than 3% of total precipitation drained in the form of stormflow runoff, despite such areas usually being associated with high saturation. During drier conditions (i.e. A and B events), which occurred over 74% of the growing season, stormflow runoff either did not occur at all (A) or was highly non-linear, only increasing significantly after the 35–36% SWC threshold was exceeded. Interestingly, a very similar SWC threshold was also found during storm conditions (C and D events). Baseflow, on the other hand, exhibited a non-linear increase when the 31%–34% SWC threshold was exceeded during both precipitation-free events (A) and storm events (C and D). Based on these observations, it would appear that this the SWC threshold value can represent a good indicator of both hydraulic slope connectivity and stormflow subsurface runoff generation, which is, in turn, closely related to water storage recharge and retention.

Previous studies have shown both similar and dissimilar SWC thresholds for different landscape, soil and climatic conditions (Radatz et al., 2013). For example, the 36% SWC threshold for stormflow runoff found in our study is very similar to that found in an experimental grassland area with sandy loam soils in Italy (Brocca et al., 2005). On the other hand, a lower 23% SWC threshold was found on the same type of soil in a small forested watershed in Canada (James & Roulet, 2007). This suggests that when SWC reaches values close to 35%, the area enters a stormflow-dominated runoff regime where rapid subsurface runoff paths become activated, first in the upper layers (for B events) then in the deepest soil layers (100 cm) during storm events (C and D events). During subsequent draining and drying of the soil, SWC falls below a ca. 31%–34% threshold and the area enters a more baseflow-dominated runoff regime. Furthermore, our data suggest that, as SWC increases during short, intense, storm events (C events), runoff coefficients increase non-linearly (Figure 5a,b), which may act as a 'push effect' in terms of area drainage; however, additional data will be needed to confirm this.

In other studies, however, highly variable results were obtained from three separate micro-catchments, with SWC threshold values ranging from 39% to 46%, the values varying widely with soil depth (Penna et al., 2011; Radatz et al., 2013; Western & Grayson, 1998). Unlike the previous studies cited, the soils in these catchments were dominated by silt loam to clay loam, allowing for zones of full

10991085, 2024, 6, Downloaded from https://onlinelibrary.wiley.com/doi/10.1002/hyp.15216 by Mendel University in Brno, Wiley Online Library on [30/06/2024]. See the Terms and Conditions (https://onlinelibrary.wiley.com/terms-and-conditions) on Wiley Online Library for rules of use; OA articles are governed by the applicable Creative Commons License

saturation to form near streams. This suggests that soil properties (soil texture and structure) are likely to have a more significant impact on SWC thresholds than climate conditions or vegetation cover, since both grassland and forest exhibited similar thresholds on the same type of soil (see above). Once again, however, additional data will be needed to confirm this hypothesis.

4.3 | Effect of rainfall on runoff generation

While there was a relatively low frequency of storm events during the growing season in this study (15 × C events, 5 × D events), they accounted for over 81% of total rainfall over the study period. Such rainfall patterns confirm the nonlinearity of current climate trends, a pattern that is predicted to get worse with ongoing climate change (Kicklighter et al., 2023). In our case, the five multiple stormflow events (D) played a significant role in restoring water levels in the catchment as they produced the lowest runoff coefficient and highest infiltration to deeper soil zones, unlike the single short-stormflow (C) events that produced the opposite results. Climate change, however, is expected to cause an increase in weather extremes (Kicklighter et al., 2023), i.e. more type C events and less type D events, which is likely to cause major problems for existing forest ecosystems (Jourdan et al., 2020) and maintaining ground water availability (Ali et al., 2011).

In our study, D events had lowest runoff coefficients and exhibited the highest ratio of infiltration to catchment water retention, as documented by high soil wetting values at 100 cm (Table 4). Moreover, baseflow runoff coefficients during D events rarely exceeded the median level, in contrast to C events (extreme rainfall) which frequently did (Figure 5a,b). This highlights the importance of longer rainy periods (i.e. multiple stormflow events) for soil water recharge. This is in accord with the findings of Radatz et al. (2013), who found that storms of longer duration were required to generate runoff in conditions where SWC is persistently low and thus does not fully saturate the soil profile, as in our own upland headwater study area. Groundwater recharge can also happen through side-flow or lateral flow (Zeng et al., 2016). Assuming that side-flow is accelerated runoff along the capillary fringe (Tanaka, 1996), its existence should be indicated in Table 4 as non-linear behaviour of SWC in the soil depth gradient. However, in event types A and B, SWC decreased with depth and conversely increased in event types D, when the whole soil profile is saturated. Non-linear behaviour could be however observed in the NT positions, which is most likely indicative of the tree effect rather than side-flow. It seems, that in the described conditions side-flow did not play a significant role in groundwater recharge.

4.4 | Methodological and interpretative aspects of the study

In this study, both runoff and SWC dynamics were compared under different rainfall-runoff event types; however, this brought a number of methodological difficulties regarding the analysis and interpretation of results. A similar methodological data mining approach was used by Juřička et al. (2022) for the analysis of rainfall infiltration affected by microrelief. Unlike Juřička et al. (2022), however, we provide additional information on actual SWC dynamics (increase/decrease) in relation to hydrological processes generated during rainfall-runoff events with different hydrological regimes. To ensure the correct interpretation of such data, however, it is essential that the different types of events are clearly delineated, particularly the end of the rainfall-affected period. While our approach was consistent with previous studies (e.g. Sumner, 1999), we provided further supporting data through direct soil measurements of saturated hydraulic conductivity (0.5 m/day) from the study area. In addition, the relatively new constant-k method (Blume et al., 2007) was used to separate stormflow runoff and baseflow (in hydrograms). Compared with other commonly used graphical separation methods (i.e. recession continued, semi-logarithmic plot, constant slope), the constant-k method (i) has been tested by Blume et al. (2007) and is theoretically supported, (ii) does not suffer from a subjective determination of the stormflow flow endpoint during rainfall-runoff events, and (iii) it can be used primarily with multiple peak events (D events). During some rainfall-runoff events in our study, however, the stormflow flow end point defined by the k-method separation was followed by subsequent increase in streamflow, which often continued into the period covered by no-rainfall A events, as evident from streamflow patterns in wet and dry antecedent conditions at the start of the growing season and during the summer (Figure 6).

We believe that this occasional streamflow increase during precipitation-free periods (A events) was caused by increasing baseflow resulting from delayed subsurface runoff from more distant parts of the headwater area. Consequently, we considered this kind of runoff behaviour as baseflow rather than stormflow for the purposes of the event analysis. At the same time, the 15-min time step has also been affected by diurnal streamflow dynamics, controlled mainly by evapotranspiration in local forest stands where streamflow naturally decreases during the day by more than to 20% and increases after sunset (Deutscher et al., 2016) which adds another level of complexity. Another role might be played by the riparian zone, which can influence the stream hydrology and discharge regime of the catchment (Lupon et al., 2016), but in our case covers less than 1% of the area.

Also, the 15-min time steps proved to be poorly visible at some of the picture's resolutions. For these reasons, we worked with baseflow runoff in daily time steps (Figure 2) which was not possible for stormflow. However, during stormflow conditions, the diurnal vegetation effect on streamflow should not be as pronounced.

Another challenge arose from the differing duration of rainfall-runoff events (0.1–11 days), which we addressed again by recalculating baseflow for the entire period to mean daily values, thereby allowing mutual comparisons on the same time scale. The same recalculation was not used for stormflow flow, however, as it never exceeded 1 day. This recalculation may have impacted the SWC threshold for runoff generation analysis and the long-term summary characteristics, which are partially defined by event duration (Table 3).

10991085, 2024, 6, Downloaded from https://onlinelibrary.wiley.com/doi/10.1002/hyp.15216 by Mendel University in Brno, Wiley Online Library on [30/06/2024]. See the Terms and Conditions (https://onlinelibrary.wiley.com/terms-and-conditions) on Wiley Online Library for rules of use; OA articles are governed by the applicable Creative Commons License

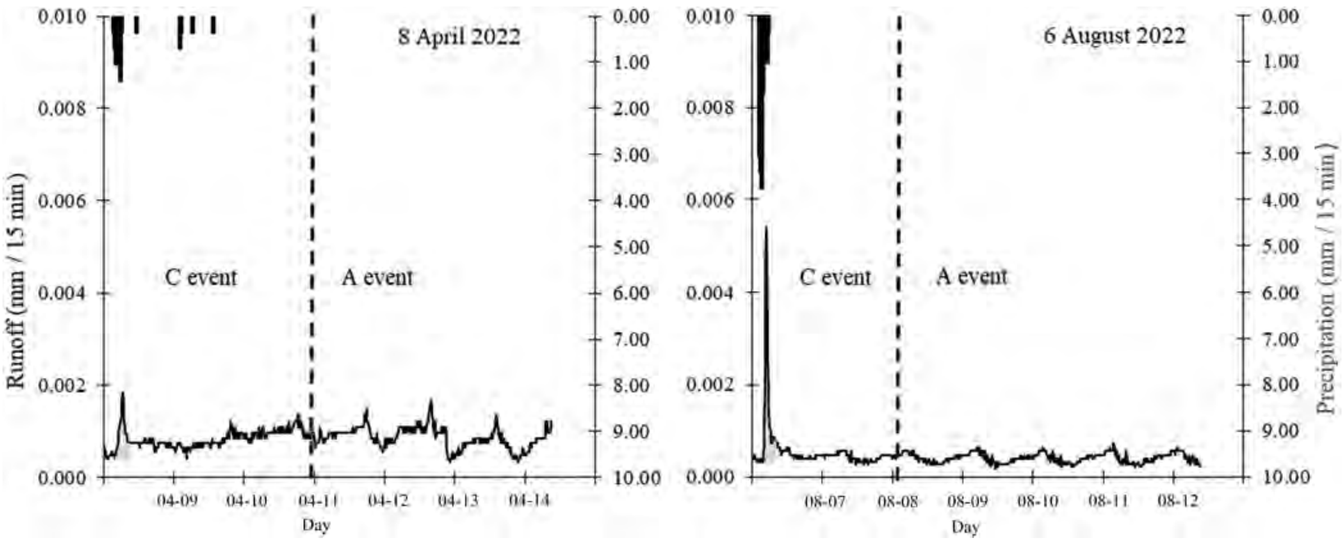

FIGURE 6 Time series for stream runoff and precipitation for (a) events with wet antecedent conditions (8 April 2022), and (b) events with dry antecedent conditions (6 August 2022). The grey area with runoff represents stormflow runoff separated by the k-constant method.

This only highlights the complexity of hydrological processes occurring at different time-scales and generated under different rainfall-runoff conditions, which is in strong contrast with the assumption that headwater catchments are simple dynamic systems, as proposed for example by Wood et al. (1988) and Kirchner (2009), after all the level of catchment complexity is still a matter of discussion (Kirchner, 2016). Indeed, the highly non-linear phenomena that characterize catchment response during rainfall events will present a challenge to most hydrological models based on assumptions of linearity (Loague et al., 2006).

In this study we concentrated on the combined effect of the forest stands neglecting the different effects individual tree species can have on the hydrological processes. SWC was measured only in stands with deciduous tree species (beech, hornbeam and oak) that were considered similar for this purpose. While beech and hornbeam exhibit similar water partitioning, oak has usually significantly more throughfall and less stemflow and can reach higher transpiration rates especially under drier conditions (Novosadová et al., 2023). Our LAI indexes as well as root density measurements indicated that the admixture of oak in these conditions did not have a clear effect on these two parameters (Table 1). Still, all the measurements were placed in mixed stands with more than one tree species so only their combined effects could be observed. While this simplified approach seems to be fine for the representation of normal climatic conditions, it is likely that both under longer wet and dry conditions, the effects of different tree species are amplified (Bittner et al., 2010) and can play a much bigger role in the alteration of the hydrological processes.

One of the important study limits is the use of single growing season dataset, which means that the presented results can be applied to a standardly wet year only. However, with the unprecedently changing conditions caused by climate change we believe that our study still holds merit and can be a valuable addition to the puzzle as a representative of standard conditions. More and longer research is needed to cover the climatic variability in different years, especially detailed microrelief survey during heavy rains to identify local sources of soil saturation, overland excess flow and variable source areas respectively.

5 | CONCLUSIONS

This study examined the hydrological response of a headwater elementary discharge area in a forested upland catchment of the Czech Republic characterized by a low hydrological response to rainfall-runoff events and high retention and water usage during the growing season (runoff coefficient 2.4%). Specifically, we examined the combined role of rainfall-runoff event type and NT and BT siting on runoff generation processes, based on 45 rainfall-runoff events and following precipitation-free periods occurring during one growing season of a standardly wet year (and growing season). The following results were obtained:

- Multiple stormflow periods (D events) were the most significant in terms of water retention and soil water recharge, since they exhibited the lowest runoff coefficient. This was in strong contrast to the hydrological response to single stormflow periods (C events), where the runoff coefficient was twice as high. We attribute this behaviour to increased vertical hydrological connectivity enabling faster transport to deeper soil layers, a process that only occurred during D events.
- The presence of trees had a significant effect on SWC dynamics during all event types; most notably during D events, where the difference between NT and BT sites reached 0.66% (NT = +0.70, BT = +0.04%), thus confirming the important role of trees in processes associated with infiltration and water redistribution to deeper soil layers.

10991085, 2024, 6, Downloaded from https://onlinelibrary.wiley.com/doi/10.1002/hyp.15216 by Mendel University in Brno, Wiley Online Library on [30/06/2024]. See the Terms and Conditions (https://onlinelibrary.wiley.com/terms-and-conditions) on Wiley Online Library for rules of use; OA articles are governed by the applicable Creative Commons License

- We described a SWC threshold of stormflow generation of 35%–36%. Values above this threshold exhibited great non-linearity, indicating the generation of stormflow runoff.
- At SWC of 31%–34%, an increased baseflow generation threshold was found indicating either the activation of quick flow paths or the hydrological connection of multiple slopes in the area. Runoff coefficients tended to increase non-linearly with increasing SWC, especially during short intense storm events (C events). This trend, which may be explained by the "push effect", identifies an important hydrological process that may be of relevance regarding the faster drainage and lower retention capacity of the area during sudden storms.

The study represents a piece of the puzzle towards a better conceptualisation of hydrological processes in elementary headwater discharge areas based on rigorous field mapping. Notably, it highlights potential widely unrecognized dangers associated with the expected increasing weather extremity associated with climate change. Under future conditions, extreme rainfalls (C events) are more likely to occur and our results indicate that events like this negatively affect soil water recharge processes and contribute to more rapid, unusable runoff.

ACKNOWLEDGEMENTS

This study was supported by the Internal Grant Scheme of Mendel University in Brno, registration no.: CZ.02.2.69/0.0/0.0/19_073/0016670, funded by the European Social Fund (ESF). We would like to thank the Training Forest Enterprise – Masaryk Forest Křtiny for providing the plots for this research, and Petr Sykora for processing LAI images. We would also like to thank Dr. Kevin Roche for his help with linguistic and stylistic correction.

CONFLICT OF INTEREST STATEMENT

The authors declare no conflicts of interest. The funders had no role in the design of the study; in the collection, analysis or interpretation of data; in the writing of the manuscript, or in the decision to publish the results. The authors also have no affiliations with, or involvement in, any organization or entity with any interest in the subject or materials discussed in this manuscript.

DATA AVAILABILITY STATEMENT

The data that support the findings of this study are available from the corresponding author upon reasonable request.

ORCID

Tomáš Vichta https://orcid.org/0000-0002-4970-002X
Jan Deutscher https://orcid.org/0000-0003-0702-7049
Ondřej Hemr https://orcid.org/0000-0002-5268-1595
Gabriela Tomášová https://orcid.org/0000-0002-9882-0829
Nikola Žižlavská https://orcid.org/0000-0001-9384-930X
Martina Brychtová https://orcid.org/0000-0001-8725-2769
Aleš Bajer https://orcid.org/0000-0001-6809-3723
Manoj Kumar Shukla https://orcid.org/0000-0002-3336-0040

REFERENCES

Ali, G. A., L'Heureux, C., Roy, A. G., Turmel, M. C., & Courchesne, F. (2011). Linking spatial patterns of perched groundwater storage and stormflow generation processes in a headwater forested catchment. *Hydrological Processes*, *25*(25), 3843–3857.

Beven, K. (1989). *Interflow. Unsaturated flow in hydrologic modeling: Theory and practice* (pp. 191–219). Springer Netherlands.

Beven, K., & Germann, P. (1982). Macropores and water flow in soils. *Water Resources Research*, *18*(5), 1311–1325.

Beven, K., & Germann, P. (2013). Macropores and water flow in soils revisited. *Water Resources Research*, *49*(6), 3071–3092.

Bittner, S., Talkner, U., Krämer, I., Beese, F., Hölscher, D., & Priesack, E. (2010). Modeling stand water budgets of mixed temperate broad-leaved forest stands by considering variations in species specific drought response. *Agricultural and Forest Meteorology*, *150*(10), 1347–1357.

Blume, T., Zehe, E., & Bronstert, A. (2007). Rainfall-runoff response, event-based runoff coefficients and hydrograph separation. *Hydrological Sciences Journal*, *52*(5), 843–862.

Böhm, W. (1979). *Methods of studying root systems* (p. 33). Springer.

Bonell, M. (1993). Progress in the understanding of runoff generation dynamics in forests. *Journal of Hydrology*, *150*(2–4), 217–275.

Brammer, D. D., & McDonnell, J. J. (1996). An evolving perceptual model of hillslopes flow at the Maimai catchment. *Advances in Hillslope Hydrology*, *1*, 35–60.

Brocca, L., Melone, F., & Moramarco, T. (2005). In F. Maraga & M. Arattano (Eds.), *Empirical and conceptual approaches for soil moisture estimation in view of event-based rainfall–runoff modeling. Progress in surface and subsurface water studies at the plot and Small Basin scale* (Vol. 77, pp. 1–8). IHP-VI, Technical Documents in Hydrology.

Carey, S. K., & Woo, M. K. (2000). The role of soil pipes as a slope runoff mechanism, subarctic Yukon, Canada. *Journal of Hydrology*, *233*(1–4), 206–222.

Chittolina, M., da Rocha, H. R., Domingues, L. M., & de Araújo Lobo, G. (2023). Hydrological response of a headwater catchment in Southeast Brazil—Threshold patterns of stormflow response. *Hydrological Processes*, *37*(5), e14879.

Czech Hydrometeorological Institute. 2023. https://www.chmi.cz/historicka-data/pocasi/zakladni-informace

Detty, J. M., & McGuire, K. J. (2010). Threshold changes in storm runoff generation at a till-mantled headwater catchment mantled headwater catchment. *Water Resources Research*, *46*, W07525.

Deutscher, J., Hemr, O., & Kupec, P. (2021). A unique approach on how to work around the common uncertainties of local field data in the PERSiST hydrological model. *Water*, *13*(9), 1143.

Deutscher, J., Kupec, P., Dundek, P., Holík, L., Machala, M., & Urban, J. (2016). Diurnal dynamics of streamflow in an upland forested micro-watershed during short precipitation-free periods is altered by tree sap flow. *Hydrological Processes*, *30*(13), 2042–2049.

Du, E., Jackson, C. R., Klaus, J., McDonnell, J. J., Griffiths, N. A., Williamson, M. F., Greco, J. L., & Bitew, M. (2016). Interflow dynamics on a low relief forested hillslope: Lots of fill, little spill. *Journal of Hydrology*, *534*, 648–658.

Farrick, K. K., & Branfireun, B. A. (2014). Soil water storage, rainfall and runoff relationships in a tropical dry forest catchment. *Water Resources Research*, *50*, 9236–9250.

Guérin, A., Devauchelle, O., Robert, V., Kitou, T., Dessert, C., Quiquerez, A., Allemand, P., & Lajeunesse, E. (2019). Stream discharge surges generated by groundwater flow. *Geophysical Research Letters*, *American Geophysical Union*, *16*, 7447–7455.

10991085, 2024, 6, Downloaded from https://onlinelibrary.wiley.com/doi/10.1002/hyp.15216 by Mendel University in Brno, Wiley Online Library on [30/06/2024]. See the Terms and Conditions (https://onlinelibrary.wiley.com/terms-and-conditions) on Wiley Online Library for rules of use; OA articles are governed by the applicable Creative Commons License

Guisan, A., Weiss, S. B., & Weiss, A. D. (1999). GLM versus CCA spatial modeling of plant species distribution. *Plant Ecology*, *143*(1), 107–122.

James, A. L., & Roulet, N. T. (2007). Investigating hydrologic connectivity and its association with threshold change in runoff response in a temperate forested watershed. *Hydrological Processes*, *21*(25), 3391–3408.

Jochheim, H., Lüttschwager, D., & Riek, W. (2022). Stem distance as an explanatory variable for the spatial distribution and chemical conditions of stand precipitation and soil solution under beech (fagus sylvatica L.) trees. *Journal of Hydrology*, *608*, 127629.

Jones, A. (1971). Soil piping and stream channel initiation. *Water Resources Research*, *7*(3), 602–610.

Jourdan, M., Kunstler, G., & Morin, X. (2020). How neighbourhood interactions control the temporal stability and resilience to drought of trees in mountain forests. *Journal of Ecology*, *108*(2), 666–677.

Juřička, D., Valtera, M., Deutscher, J., Vichta, T., Pecina, V., Patočka, Z., … Pařílková, J. (2022). The role of pit-mound microrelief in the redistribution of rainwater in forest soils: A natural legacy facilitating groundwater recharge? *European Journal of Forest Research*, *141*(2), 321–345.

Kicklighter, D. W., Lin, T. S., Zhang, J., Chen, M., Vörösmarty, C. J., Jain, A. K., & Melillo, J. M. (2023). Influence of forest infrastructure on the responses of ecosystem services to climate extremes in the Midwest and Northeast United States from 1980 to 2019. Frontiers in environmental. *Science*, *11*.

Kirchner, J. W. (2009). Catchments as simple dynamical systems: Catchment characterization, rainfall-runoff modeling, and doing hydrology backward. *Water Resources Research*, *45*(2), W02429.

Kirchner, J. W. (2016). Aggregation in environmental systems – part 1: Seasonal tracer cycles quantify young water fractions, but not mean transit times, in spatially heterogeneous catchments. *Hydrology and Earth System Sciences*, *20*(1), 279–297.

Kitahara, H., & Nakai, Y. (1992). Relationship of pipe flow to streamflow on a first order watershed. *Journal of the Japanese Forestry Society*, *74*(1), 49–54.

Kitahara, H., Terajima, T., & Nakai, Y. (1994). Ratio of pipe flow to throughflow discharge. *Journal of the Japanese Forestry Society*, *76*(1), 10–17.

Lal, R. (1987). Tropical ecology and physical edaphology.

Lee, E., & Kim, S. (2020). Characterization of runoff generation in a mountainous hillslope according to multiple threshold behavior and hysteretic loop features. *Journal of Hydrology*, *590*, 125534.

Liang, W. L., Kosugi, K. I., & Mizuyama, T. (2011). Soil water dynamics around a tree on a hillslope with or without rainwater supplied by stemflow. *Water Resources Research*, *47*(2), W02541.

Loague, K., Heppner, C. S., Mirus, B. B., Ebel, B. A., Carr, A. E., BeVille, S. H., & Vander Kwaak, J. E. (2006). Physics-based hydrologic-response simulation: Foundation for hydroecology and hydrogeomorphology. *Hydrological Processes*, *20*, 1231–1237.

Lupon, A., Bernal, S., Poblador, S., Martí, E., & Sabater, F. (2016). The influence of riparian evapotranspiration on stream hydrology and nitrogen retention in a subhumid Mediterranean catchment. *Hydrology and Earth System Sciences*, *20*, 3831–3842.

McGlynn, B. L. (2005). The role of riparian zones in steep mountain watersheds, The role of riparian zones in Steep Mountain watersheds. In *Global change and mountain regions: An overview of current knowledge* (pp. 331–342). Springer.

McGlynn, B. L., McDonnell, J. J., Seibert, J., & Kendall, C. (2004). Scale effects on headwater catchment runoff timing, flow sources, and groundwater-streamflow relations. *Water Resources Research*, *40*(7), W07504.

Metzger, J. C., Filipzik, J., Michalzik, B., & Hildebrandt, A. (2021). Stemflow infiltration hotspots create soil microsites near tree stems in an unmanaged mixed beech forest. *Frontiers in Forests and Global Change*, *4*, 701293.

Norbiato, D., & Borga, M. (2008). Analysis of hysteretic behaviour of a hillslope-storage kinematic wave model for subsurface flow. *Advances in Water Resources*, *31*(1), 118–131.

Novosadová, K., Kadlec, J., Řehořková, Š., Matoušková, M., Urban, J., & Pokorný, R. (2023). Comparison of rainfall partitioning and estimation of the utilisation of available water in a monoculture beech Forest and a mixed beech-oak-Linden Forest. *Water*, *15*(2), 285.

Nyman, P., Sheridan, G., & Lane, P. N. J. (2010). Synergistic effects ofwater repellency and macropore flow on the hydraulic conductivity ofa burned forest soil, south-east Australia. *Hydrological Processes*, *24*, 2871–2887.

Ocampo, C. J., Sivapalan, M., & Oldham, C. (2006). Hydrological connectivity of upland-riparian zones in agricultural catchments: Implications for runoff generation and nitrate transport. *Journal of Hydrology*, *331*(3–4), 643–658.

Penna, D., Tromp-van Meerveld, H. J., Gobbi, A., Borga, M., & Dalla Fontana, G. (2011). The influence of soil moisture on threshold runoff generation processes in an alpine headwater catchment. *Hydrology and Earth System Sciences*, *15*(3), 689–702.

R Core Team. (2017). R: A language and environment for statistical computing; R foundation for statistical computing, Vienna, Austria. http://www.R-project.org/

Radatz, T. F., Thompson, A. M., & Madison, F. W. (2013). Soil moisture and rainfall intensity thresholds for runoff generation in southwestern Wisconsin agricultural watersheds. *Hydrological Processes*, *27*(25), 3521–3534.

Roberge, J., & Plamondon, A. P. (1987). Snowmelt runoff pathways in a boreal forest hillslope, the role of pipe throughflow. *Journal of Hydrology*, *95*(1–2), 39–54.

Roberts, J. (2000). The influence of physical and physiological characteristics of vegetation on their hydrological response. *Hydrological Processes*, *14*(16–17), 2885–2901.

Scaife, C. I., Singh, N. K., Emanuel, R. E., Miniat, C. F., & Band, L. E. (2020). Non-linear quickflow response as indicators of runoff generation mechanisms. *Hydrological Processes*, *34*(13), 2949–2964.

Schellekens, J., Scatena, F. N., Bruijnzeel, L. A., Van Dijk, A. I. J. M., Groen, M. M. A., & Van Hogezand, R. J. P. (2004). Stormflow generation in a small rainforest catchment in the Luquillo experimental forest, Puerto Rico. *Hydrological Processes*, *18*(3), 505–530.

Sidle, R. C., Tsuboyama, Y., Noguchi, S., Hosoda, I., Fujieda, M., & Shimizu, T. (1995). Seasonal hydrologic response at various spatial scales in a small forested catchment, Hitachi Ohta, Japan. *Journal of Hydrology*, *168*(1–4), 227–250.

Sidle, R. C., Tsuboyama, Y., Noguchi, S., Hosoda, I., Fujieda, M., & Shimizu, T. (2000). Stormflow generation in steep forested headwaters: A linked hydrogeomorphic paradigm. *Hydrological Processes*, *14*(3), 369–385.

Staelens, J., De Schrijver, A., Verheyen, K., & Verhoest, N. E. C. (2008). Rainfall partitioning into throughfall, stemflow, and interception within a single beech (fagus sylvatica L.) canopy: Influence of foliation, rain event characteristics, and meteorology. *Hydrological Processes*, *22*(1), 33–45.

Sumner, M. E. (Ed.). (1999). *Handbook of soil science*. CRC press.

Tanaka, T. (1996). Rainwater percolation and groundwater recharge. 4. Natural recharge of groundwater (process of natural recharge); Usui shinto to chikasui kanyo. 4. Chikasui no shizen kanyo (shizen kanyo process). Chikasui Gakkaishi. *Journal of Groundwater Hydrology*, *38*.

Tetzlaff, D., McDonnell, J. J., Uhlenbrook, S., McGuire, K. J., Bogaart, P. W., Naef, F., Baird, A. J., Dunn, S. M., & Soulsby, C. (2008). Conceptualizing catchment processes: Simply too complex? *Hydrological Processes*, *22*(11), 1727–1730.

Tromp-Meerveld, H. J., & McDonnell, J. J. (2005). Comment to "spatial correlation of soil moisture in small catchments and its relationship to dominant spatial hydrological processes, journal of hydrology 286: 113–134". *Journal of Hydrology*, *303*(1–4), 307–312.

10991085, 2024, 6, Downloaded from https://onlinelibrary.wiley.com/doi/10.1002/hyp.15216 by Mendel University in Brno, Wiley Online Library on [30/06/2024]. See the Terms and Conditions (https://onlinelibrary.wiley.com/terms-and-conditions) on Wiley Online Library for rules of use; OA articles are governed by the applicable Creative Commons License

Tromp-Van Meerveld, H. J., & McDonnell, J. J. (2006). Threshold relations in subsurface stormflow: 2. The fill and spill hypothesis. *Water Resources Research*, *42*(2), W02411.

Uchida, T., Tromp-van Meerveld, I., & McDonnell, J. J. (2005). The role of lateral pipe flow in hillslope runoff response: An intercomparison of non-linear hillslope response. *Journal of Hydrology*, *311*(1–4), 117–133.

USDA. (1999). Soil taxonomy: A basic system of soil classification for making and interpreting soil surveys. In USDA (Ed.), *Agriculture Handbook* (Vol. 436, 2nd ed.). Govt. Printer.

Wei, L., Qiu, Z., Zhou, G., Kinouchi, T., & Liu, Y. (2020). Stormflow threshold behaviour in a subtropical mountainous headwater catchment during forest recovery period. *Hydrological Processes*, *34*(8), 1728–1740.

Weiler, M. (2016). Macropores and preferential flow – A love-hate relationship. *Hydrological Processes*, *31*, 15–19.

Weiss, A. (2001). Topographic position and landforms analysis. In *Poster presentation, ESRI user conference* (Vol. 200). ESRI Press.

Wenninger, J., Uhlenbrook, S., Tilch, N., & Leibundgut, C. (2004). Experimental evidence of fast groundwater responses in a hillslope/floodplain area in the Black Forest Mountains, Germany. *Hydrological Processes*, *18*(17), 3305–3322.

Western, A. W., & Grayson, R. B. (1998). The Tarrawarra data set: Soil moisture patterns, soil characteristics, and hydrological flux measurements. *Water Resources Research*, *34*(10), 2765–2768.

Wild, J., Kopecký, M., Macek, M., Šanda, M., Jankovec, J., & Haase, T. (2019). Climate at ecologically relevant scales: A new temperature and soil moisture logger for long-term microclimate measurement. *Agricultural and Forest Meteorology*, *268*, 40–47.

Wilson, G. V., Nieber, J. L., Fox, G. A., Dabney, S. M., Ursic, M., & Rigby, J. R. (2017). Hydrologic connectivity and threshold behavior of hillslopes with fragipans and soil pipe networks. *Hydrological Processes*, *31*, 2477–2496.

Wood, E. F., Sivapalan, M., Beven, K., & Band, L. (1988). Effects of spatial variability and scale with implications to hydrologic modeling. *Journal of Hydrology*, *102*(1–4), 29–47.

WRB. (2014). World Reference Base for soil resources 2014. In *International Soil Classification System for Naming Soils and Creating Legends for Soil Maps*, 1st ed.;World Soil Resources Reports No. 106; FAO: Rome, Italy, 2014; p. 203.

Zehe, E., Elsenbeer, H., Lindenmaier, F., Schulz, K., & Blöschl, G. (2007). Patterns of predictability in hydrological threshold systems. *Water Resources Research*, *43*(7), W07434.

Zehe, E., & Sivapalan, M. (2009). Threshold behaviour in hydrological systems as (human) geo-ecosystems: Manifestations, controls, implications. *Hydrology and Earth System Sciences*, *13*(7), 1273–1297.

Zeng, Y., Xie, Z., Yu, Y., Liu, S., Wang, L., Zou, J., & Jia, B. (2016). Effects of anthropogenic water regulation and groundwater lateral flow on land processes. *Journal of Advances in Modeling Earth Systems*, *8*(3), 1106–1131.

SUPPORTING INFORMATION

Additional supporting information can be found online in the Supporting Information section at the end of this article.

How to cite this article: Vichta, T., Deutscher, J., Hemr, O., Tomášová, G., Žižlavská, N., Brychtová, M., Bajer, A., & Shukla, M. K. (2024). Combined effects of rainfall-runoff events and antecedent soil moisture on runoff generation processes in an upland forested headwater area. *Hydrological Processes*, *38*(6), e15216. https://doi.org/10.1002/hyp.15216

10991085, 2024, 6, Downloaded from https://onlinelibrary.wiley.com/doi/10.1002/hyp.15216 by Mendel University in Brno, Wiley Online Library on [30/06/2024]. See the Terms and Conditions (https://onlinelibrary.wiley.com/terms-and-conditions) on Wiley Online Library for rules of use; OA articles are governed by the applicable Creative Commons License